Real-Time LiDAR SLAM-Driven Navigation and Collision Avoidance for Mobile Robots in Unstructured Environments

Amandyk Tuleshov[1], Anar Adilkhan[2], Moldir Kuatova[3], Gaukhar Seidaliyeva[4]
Joldasbekov Institute of Mechanics and Engineering, Almaty, Kazakhstan[1, 2, 3]
University of International Business, Almaty, Kazakhstan[4]

***Abstract*—Autonomous navigation in unknown environments requires accurate simultaneous localization and mapping, reliable obstacle detection, and efficient path planning within a unified framework. This study proposes a real-time LiDAR-based SLAM-driven navigation system for mobile robots operating in structured indoor environments. The developed architecture integrates three-dimensional LiDAR sensing, ego-motion estimation, scan registration, loop closure optimization, and collision-aware trajectory planning to achieve robust environmental reconstruction and safe autonomous mobility. A probabilistic measurement model is employed to relate sensor observations to robot pose and map states, while back-end optimization mitigates cumulative drift and enhances global consistency. The navigation module incorporates obstacle segmentation and goal-directed path generation, ensuring smooth and collision-free trajectories under kinematic constraints. Experimental validation is conducted in both incremental and full-environment exploration scenarios using a physical robotic platform equipped with LiDAR and auxiliary sensors. Results demonstrate consistent mapping accuracy, stable trajectory estimation, and effective obstacle avoidance in cluttered indoor settings. The system maintains real-time computational performance while preserving the structural coherence of reconstructed environments. The findings confirm the reliability and scalability of the proposed framework, providing a practical foundation for autonomous robotic navigation in semi-structured and unstructured operational domains.**

Keywords*—*LiDAR SLAM; autonomous navigation; obstacle avoidance; path planning; mobile robots; real-time mapping; 3D point cloud processing; loop closure optimization; sensor fusion; robotic perception

I. Introduction

Autonomous mobile robots are increasingly expected to operate reliably in complex and previously unknown environments, where accurate perception and safe motion planning are essential for mission success. The integration of sensing, localization, and navigation modules has therefore become a central research focus in intelligent robotics. Among various sensing technologies, Light Detection and Ranging (LiDAR) has demonstrated strong capability in providing high-resolution geometric information that supports robust environmental understanding under diverse lighting and weather conditions [1]. As illustrated in Fig. 1, LiDAR-driven navigation pipelines enable robots to perceive surrounding structures and generate actionable spatial representations for decision making.

Simultaneous Localization and Mapping (SLAM) plays a fundamental role in enabling autonomy in unknown environments by allowing robots to build maps while continuously estimating their own pose. Conventional localization methods that rely on pre-built maps are often unsuitable for dynamic or unexplored settings. In contrast, SLAM frameworks provide adaptive mapping capabilities that improve operational flexibility and scalability [2]. However, early SLAM techniques frequently suffered from accumulated drift and sensitivity to sensor noise, which limited their effectiveness in long-term deployments [3]. Recent LiDAR-based SLAM approaches have addressed many of these issues through improved scan matching strategies, loop closure mechanisms, and graph optimization techniques that enhance global consistency [4].

Fig. 1. Overall architecture of a real-time LiDAR SLAM-driven navigation and collision avoidance framework for mobile robots.

While accurate mapping is necessary, it is not sufficient for safe autonomy. Real-time obstacle detection and collision avoidance must be tightly integrated with the localization

pipeline to ensure reliable navigation performance. In many real-world scenarios, mobile robots encounter dynamic obstacles, irregular terrain, and partially observable environments. Traditional path planning methods, including grid-based search and sampling-based planners, can produce feasible trajectories but often struggle with computational efficiency or rapid environmental changes [5]. Consequently, modern robotic systems increasingly adopt unified frameworks that couple perception with reactive planning modules to improve responsiveness and safety [6]. Fig. 1 conceptually depicts this tight coupling between mapping, obstacle detection, and motion planning components.

Another important consideration is computational efficiency under real-time constraints. Processing dense LiDAR scans, updating maps, and generating collision-free trajectories require significant computational resources. Systems that fail to meet timing requirements may exhibit delayed reactions that compromise safety. Therefore, lightweight and optimized navigation architectures have become a major research priority, particularly for embedded robotic platforms with limited onboard computation [7]. Furthermore, unstructured environments such as warehouses, outdoor terrains, and disaster response zones introduce significant uncertainty, requiring navigation systems that remain robust under incomplete or noisy observations [8].

Motivated by these challenges, this study proposes a real-time LiDAR SLAM-driven navigation framework designed to enhance obstacle avoidance and path planning performance in unknown environments. The proposed system emphasizes tight module integration, efficient data processing, and reliable collision prevention, as conceptually illustrated in Fig. 1. By improving both perception fidelity and planning responsiveness, the presented approach aims to advance the practical deployment of autonomous mobile robots in complex and dynamically changing operational scenarios [9].

II. Problem Statement

Recent advances in autonomous mobile robotics have produced a wide spectrum of LiDAR-based SLAM and navigation solutions, reflecting the growing demand for reliable operation in unknown and unstructured environments. As summarized in Fig. 2, existing research can be broadly categorized into LiDAR-based SLAM techniques, obstacle avoidance strategies, and path planning methodologies. Each category has evolved significantly, yet important challenges remain in achieving fully integrated and real-time performance.

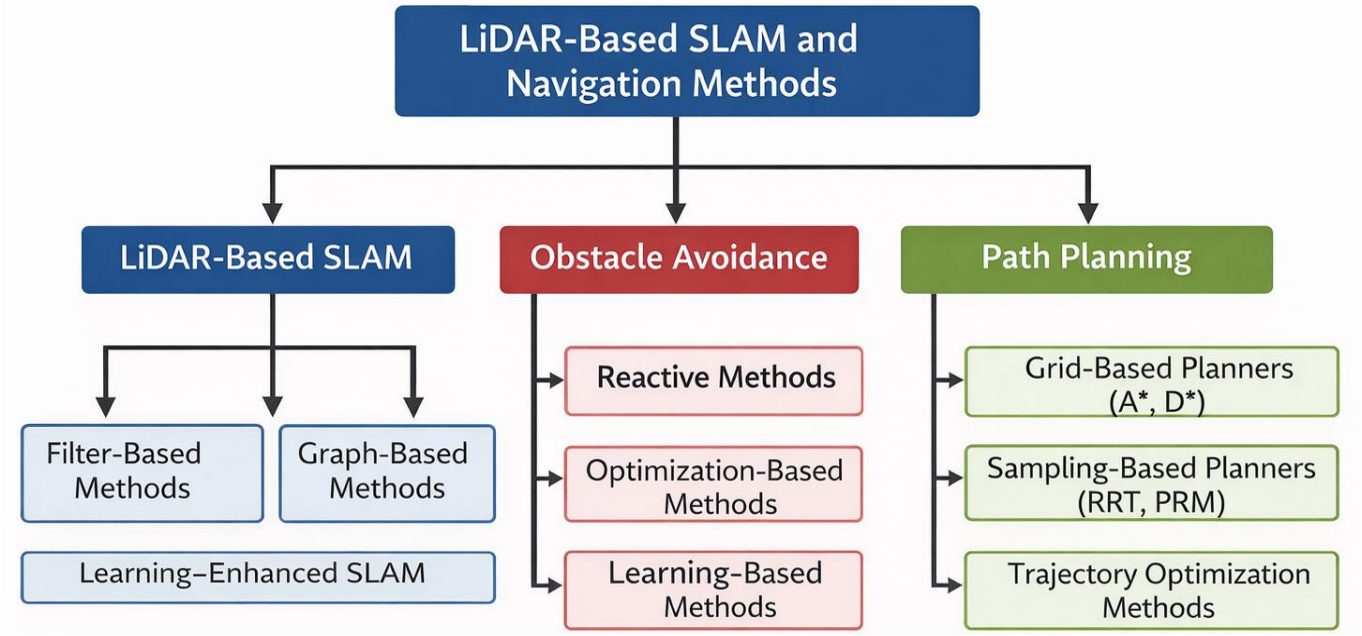

Fig. 2. Taxonomy of LiDAR-based SLAM and navigation methods for mobile robots.

Early LiDAR SLAM systems primarily relied on filter-based estimation frameworks that used probabilistic inference to update robot pose and map representations incrementally [10]. These approaches demonstrated solid theoretical foundations but often suffered from linearization errors and scalability limitations in large environments [11]. To address these issues, graph-based SLAM formulations were introduced, enabling global optimization through pose graph refinement and loop closure detection [12]. Such methods significantly improved mapping consistency over long trajectories and became widely adopted in modern robotic platforms [13]. More recently, learning enhanced SLAM paradigms have emerged, incorporating deep feature extraction and data-driven scan matching to improve robustness in perceptually challenging environments [14].

In parallel, obstacle avoidance research has progressed from purely reactive control policies toward more predictive and optimization-driven solutions. Classical reactive methods provided fast responses using local sensor information but often led to suboptimal or oscillatory behaviour in cluttered spaces [15]. Optimization based avoidance frameworks improved trajectory smoothness and safety margins by explicitly modeling robot dynamics and environmental constraints [16]. However, these methods often require substantial computational resources,

which can limit real-time deployment on embedded systems [17]. Learning based avoidance strategies have therefore gained attention, enabling robots to infer collision-free behaviors from experience and adapt to complex dynamic scenes [18].

Path planning represents another critical component of autonomous navigation. Grid-based planners such as A and D star algorithms remain popular due to their completeness and deterministic behavior in structured environments [19]. Nevertheless, their computational burden increases rapidly with map resolution and environmental scale [20]. Sampling-based planners, including RRT and PRM, have been widely adopted to address high-dimensional planning problems, offering probabilistic completeness and improved scalability [21]. Despite these advantages, such planners may produce dynamically infeasible or suboptimal trajectories without additional smoothing or optimization stages [22]. Trajectory optimization methods have therefore been proposed to generate dynamically consistent and smooth paths while satisfying kinematic constraints [23].

Although substantial progress has been achieved across these domains, many existing systems still treat mapping, obstacle avoidance, and planning as loosely coupled modules [24]. This separation can introduce latency and reduce robustness when robots operate in highly dynamic environments [25]. Recent research trends emphasize tightly integrated navigation architectures that fuse perception and planning within unified frameworks [26]. Such integration has shown improved responsiveness and safety in complex scenarios [27]. However, achieving real-time performance while maintaining mapping accuracy and planning reliability remains an open research challenge [28]. Furthermore, many current approaches are evaluated primarily in structured indoor settings, limiting their generalization to unstructured environments [29].

To address these limitations, the present work builds upon the taxonomy illustrated in Fig. 2 and proposes a tightly coupled LiDAR SLAM-driven navigation framework designed for real-time operation in unknown environments. By combining robust mapping, efficient obstacle detection, and responsive path planning, the proposed approach aims to overcome the fragmentation observed in prior systems and advance the practical deployment of autonomous mobile robots [30-34].

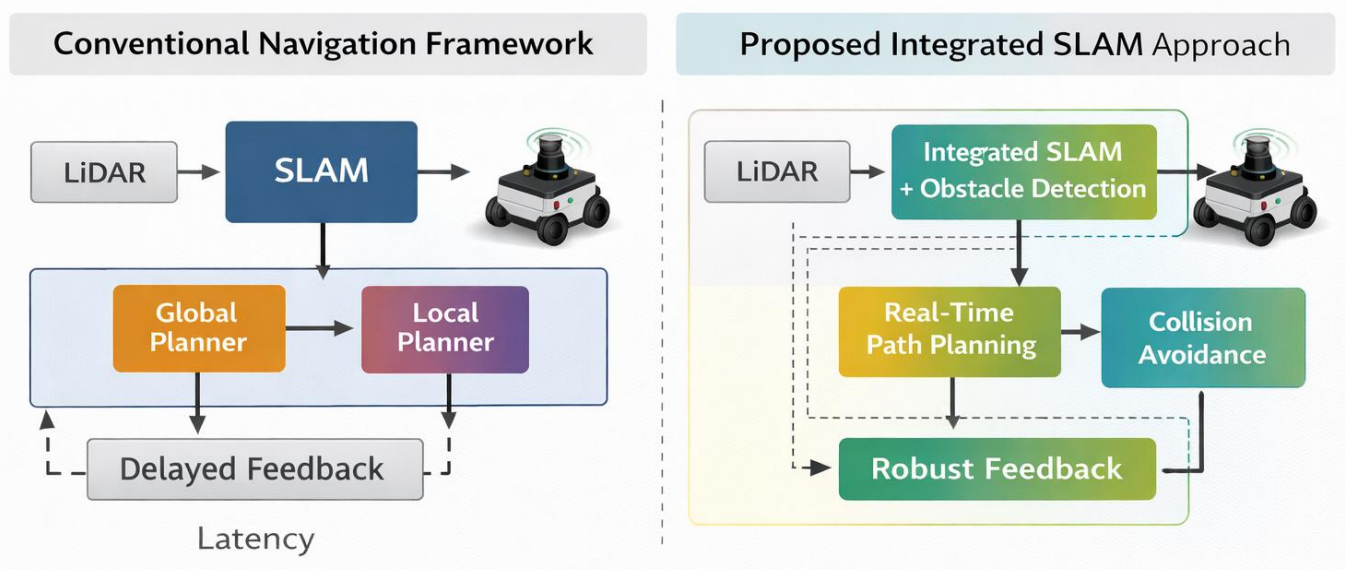

Fig. 3. Comparative pipeline of conventional navigation frameworks versus the proposed integrated SLAM approach.

Fig. 3 highlights the structural differences between conventional navigation pipelines and more recent integrated SLAM-driven approaches. In traditional architectures, perception, global planning, and local planning are typically organized as sequential and loosely coupled modules. This design simplifies implementation but often introduces latency due to delayed feedback loops between mapping and motion control components. As shown on the left side of Fig. 3, the reliance on separate global and local planners can lead to slower reaction times when the robot encounters unexpected obstacles. Such limitations become particularly pronounced in dynamic or partially observable environments where timely decision-making is critical for safe navigation.

In contrast, the integrated framework illustrated on the right side of Fig. 3 reflects a growing research trend toward tightly coupled perception and planning systems. By embedding obstacle detection directly within the SLAM pipeline and enabling real-time path replanning, modern approaches aim to reduce computational delay and improve responsiveness. The presence of robust feedback loops allows the robot to continuously refine its trajectory based on updated environmental information, thereby enhancing collision avoidance performance. This architectural shift demonstrates the importance of unified navigation strategies that jointly optimize localization accuracy, environmental awareness, and motion safety in complex unstructured environments.

Autonomous navigation of mobile robots in unknown and unstructured environments remains a challenging problem due to the simultaneous requirements of accurate localization, reliable mapping, and safe motion planning [35]. In practical deployments, robots must operate under incomplete observations, dynamic obstacles, and strict real-time constraints.

These factors often lead to accumulated drift, inconsistent map representations, and delayed collision responses [36]. Consequently, the core problem addressed in this study is the development of a tightly coupled navigation framework that ensures both geometric accuracy and motion safety while maintaining computational efficiency.

Formally, the navigation problem can be expressed as a joint estimation and control task. Given a sequence of LiDAR observations $z_{1:t}$ and control inputs $u_{1:t}$, the robot must estimate its pose x_t and the environment map m by maximizing the posterior probability.

$$(x_t^*, m^*) = arg \max_{x_t, m} p(x_t, m | z_{1:t}, u_{1:t}) \quad (1)$$

In highly unstructured environments, this estimation becomes unstable due to sensor noise and environmental ambiguity. Errors in pose estimation propagate directly into the planning layer, increasing the risk of unsafe trajectories. Therefore, localization and mapping accuracy directly influence downstream navigation reliability.

Beyond state estimation, the robot must generate a collision-free trajectory toward a goal position x_g . Let the planned path be denoted by $\tau = \{x_1, x_2, \dots, x_T\}$. The path planning objective can be formulated as a constrained optimization problem

$$\tau^* = arg \min_{\tau} J(\tau) \; subject \; to \; d(x_t, O) \geq d_{safe}, \forall t \quad (2)$$

Where $J(\tau)$ represents a composite cost including path length, smoothness, and control effort, O denotes the set of obstacles, and d_{safe} is the minimum safety margin. In dynamic environments, maintaining this constraint in real time is particularly difficult because obstacle positions may change faster than the planner can react.

To explicitly account for responsiveness, the navigation system must also satisfy a real-time feasibility condition. Let T_{proc} denote the total processing latency of perception and planning, and T_{proc} represent the maximum allowable reaction time for safe avoidance. The system must satisfy

$$T_{proc} \leq T_{react} \quad (3)$$

Otherwise, the robot may fail to avoid imminent collisions. Many existing pipelines violate this condition due to loosely coupled modules and delayed feedback loops. Therefore, the fundamental research problem is to design an integrated LiDAR SLAM-driven navigation framework that simultaneously minimizes estimation error, guarantees collision-free motion, and satisfies real-time computational constraints in unknown and dynamically evolving environments.

III. Materials and Methods

This section presents the proposed integrated LiDAR SLAM-driven navigation framework for real-time obstacle avoidance and path planning in unstructured environments. The overall methodology is structured around sensor selection, motion modeling, measurement formulation, state estimation, environmental representation, and hierarchical planning. Moreover, this section collectively illustrates the sensing configuration, mathematical modeling, and system-level architecture.

A. Sensor Configuration and Data Acquisition

The navigation system employs a heterogeneous sensing setup consisting of monocular or stereo cameras, an inertial measurement unit, and a 3D LiDAR sensor, as illustrated in Fig. 4. The camera subsystem provides visual features useful for structural reconstruction and loop closure detection. The inertial measurement unit supplies angular velocity and linear acceleration measurements for short-term motion prediction. The 3D LiDAR sensor produces dense point clouds that capture geometric properties of the surrounding environment.

Fig. 4. Multi-sensor configuration for mobile robot navigation including camera, IMU, and 3D LiDAR modules.

The integration of multiple sensing modalities increases robustness under varying illumination and environmental conditions. Fig. 4 highlights the complementary roles of each sensor type, where LiDAR ensures accurate distance measurement, the IMU enhances motion continuity, and cameras provide semantic and structural cues.

B. Ego Motion and Environmental Representation

The ego motion of the mobile robot is modeled as a three-dimensional state vector including position, orientation, and velocity.

Fig. 5. Ego-motion estimation and 3D environmental representation framework for mobile robot localization and mapping.

As depicted in Fig. 5, the robot motion is represented by translational and rotational components in Cartesian space. The resulting motion model is expressed as:

$$x_k = f(x_{k-1}, u_k) + w_k \quad (4)$$

Where x_k denotes the state vector at time k, u_k represents control input derived from encoder and IMU data, w_k and denotes process noise.

The structural representation of the environment is constructed from accumulated LiDAR point clouds, forming either a voxel grid or an occupancy map. Fig. 5 emphasizes the relationship between ego motion estimation and 3D mapping.

C. Measurement Model

The observation process is mathematically formulated as shown in Fig. 6, where the sensor output is modeled as:

$$x_k = f(x_{k-1}, u_k) + w_k \quad (5)$$

Here, z denotes the sensor measurement, x represents the robot state, m denotes the map, κ corresponds to calibration parameters, and ϵ_k is measurement noise.

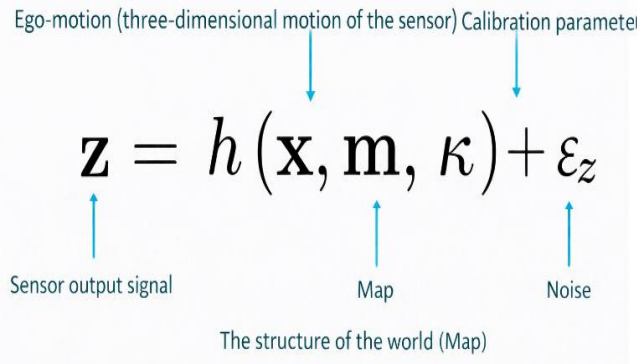

Fig. 6. Probabilistic Measurement Model Relating Sensor Observations, Robot State, Map, and Calibration Parameters

This formulation captures the dependency of LiDAR returns on both robot pose and environmental structure. Calibration parameters ensure consistency between the coordinate frames of the LiDAR, IMU, and robot base.

D. SLAM Estimation Framework

The complete SLAM estimation process is depicted in Fig. 7, where multiple measurements z_1, z_2, …, z_N are processed within the SLAM system to estimate optimized state variables $\hat{x}, \hat{m}, \hat{k}$.

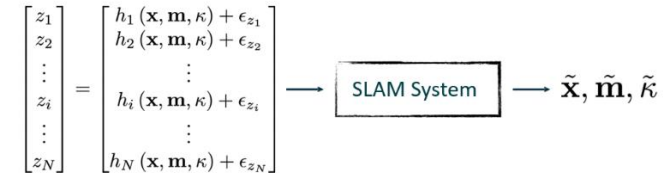

Fig. 7. Nonlinear SLAM Estimation Framework for Joint Optimization of State, Map, and Calibration Variables

The estimation is performed through nonlinear optimization by minimizing the residual error:

$$\min_{x,m} \sum_{i=1}^{N} \|x_i - h_i(x, m, k)\|^2 \quad (5)$$

This approach reduces cumulative drift and improves global consistency. The SLAM backend integrates odometry, scan matching, and loop closure constraints to generate a consistent global map.

E. Sensor Impact on Mapping Strategy

Fig. 8 illustrates how different sensing modalities affect mapping representation. Photogrammetric approaches produce sparse point clouds dependent on visual texture. Two-dimensional LiDAR yields planar occupancy maps suitable for structured indoor environments. In contrast, 3D LiDAR provides dense volumetric representations capable of handling uneven terrain and complex geometries.

For this study, 3D LiDAR is selected to enable robust perception in unstructured environments, where height variation and irregular obstacles are present.

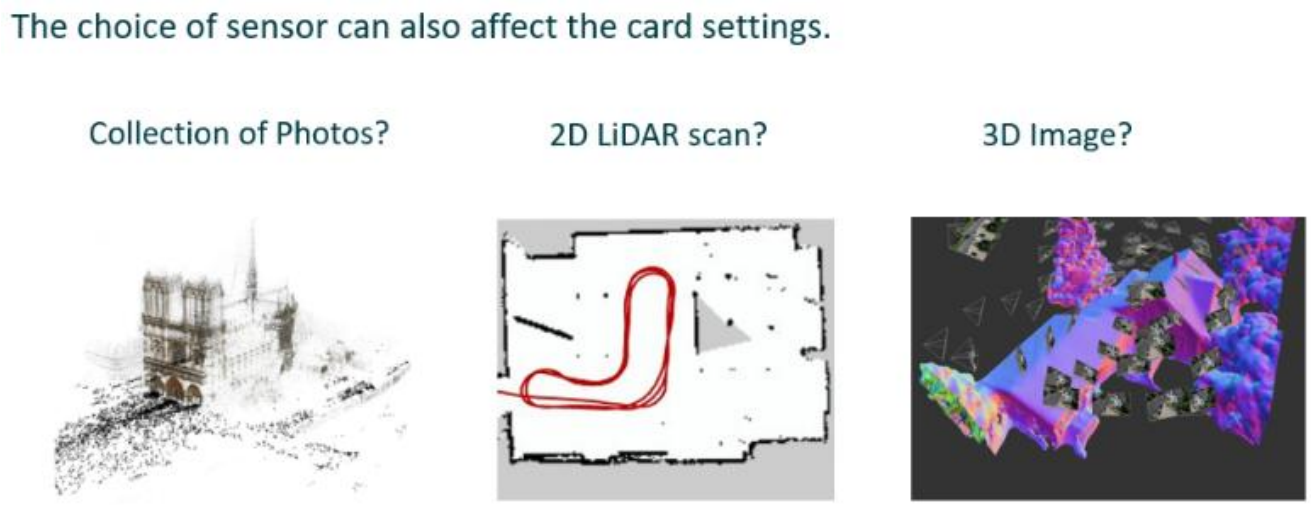

Fig. 8. Comparative impact of sensor modalities on environmental representation and mapping strategy.

F. Integrated Navigation Architecture

The integrated navigation architecture, illustrated in Fig. 9, represents a tightly coupled closed-loop framework that unifies perception, mapping, and motion planning within a single operational pipeline. The system begins with the 3D LiDAR perception module, which generates dense point cloud data representing the surrounding environment. These raw measurements undergo geometric filtering and segmentation to extract structural features such as walls and obstacles. Simultaneously, encoder readings and inertial measurement unit outputs provide incremental motion information, contributing to odometry estimation and short-term pose prediction. The fusion of LiDAR-based scan matching with proprioceptive motion data enhances robustness against drift and transient sensor noise.

The mapping module functions in a continuous update cycle to improve the accuracy of the robot's global pose estimation while simultaneously refining the environmental model. Incoming LiDAR scans are incrementally registered against

previously stored data, enabling consistent map expansion as exploration progresses. Back-end optimization techniques, including pose graph refinement and loop closure correction, are employed to reduce cumulative drift and mitigate long-term localization errors. This process ensures structural coherence and geometric alignment across extended trajectories. The finalized map provides a reliable spatial reference that supports precise path planning, obstacle avoidance, and stable autonomous navigation decisions.

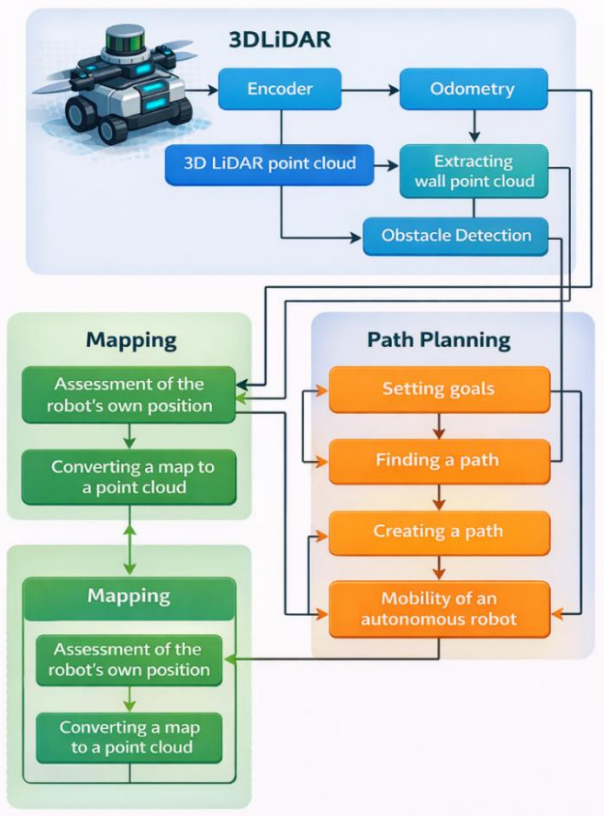

Fig. 9. Integrated 3D LiDAR-based navigation architecture incorporating perception, mapping, and path planning modules.

The planning subsystem follows a hierarchical structure comprising goal definition, path search, trajectory generation, and motion execution. Global path computation determines a collision-free route toward the designated target, while local trajectory optimization enforces kinematic feasibility and safety constraints. Obstacle detection outputs are directly transmitted to the planning layer, enabling real-time trajectory adaptation in response to environmental changes. This bidirectional feedback mechanism ensures that control commands are continuously adjusted according to updated sensor observations, thereby maintaining stable, collision-free, and responsive autonomous navigation in dynamic environments.

G. Path Planning Strategy

Path planning is divided into global and local components. The global planner computes a collision-free path using grid-based search. The local planner performs trajectory optimization considering the dynamic constraints of the robot.

The cost function used in local trajectory generation is expressed as:

$$J = \alpha J_{path} + \beta J_{obs} + \gamma J_{smooth} \quad (6)$$

Where J_{path} penalizes deviation from the global path, J_{obs} represents obstacle proximity cost, and J_{smooth} enforces trajectory smoothness. Coefficients α, β, γ balance navigation objectives.

The system is implemented within a robotics middleware framework, enabling real-time message passing between modules. Point cloud processing is accelerated using parallel computation. The planning module operates at a higher frequency than global mapping to ensure rapid obstacle avoidance.

The proposed framework integrates multi-sensor perception, probabilistic SLAM estimation, volumetric mapping, and hierarchical planning into a unified navigation architecture. The figures in this section collectively demonstrate the sensing configuration, mathematical modeling, estimation structure, and integrated execution pipeline. This tightly coupled design enables robust localization, accurate mapping, and responsive obstacle avoidance in complex unstructured environments.

IV. Experimental Results

This section presents a comprehensive experimental evaluation of the proposed LiDAR-based SLAM, obstacle avoidance, and path planning framework under both simulated and real-world indoor conditions. The experiments are designed to assess mapping accuracy, trajectory consistency, collision-free navigation capability, and system stability during autonomous operation. Quantitative and qualitative analyses are conducted using incremental mapping sequences, full-environment reconstruction, and real-time navigation trials in cluttered laboratory settings. The presented results demonstrate the effectiveness of sensor fusion, pose estimation refinement, and integrated planning modules in generating geometrically consistent maps and smooth navigation trajectories. Furthermore, performance is examined at different exploration stages, including initialization, partial mapping, and full-environment coverage, to evaluate robustness against drift accumulation and environmental complexity. The findings provide empirical evidence supporting the reliability and scalability of the proposed framework for autonomous mobile robotic applications.

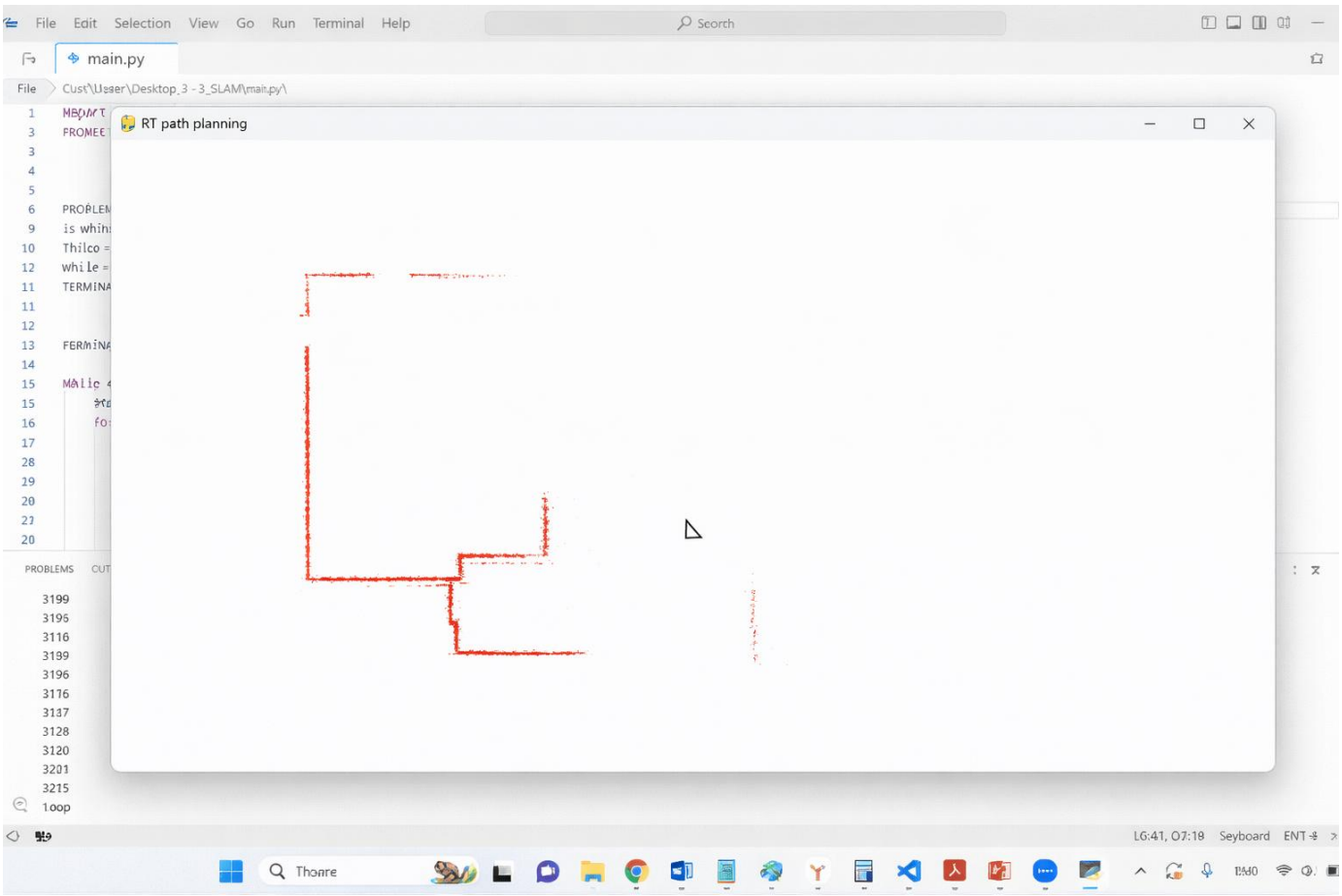

Fig. 10. Initialization phase of the LiDAR-based SLAM process showing partial environmental reconstruction.

Fig. 10 depicts the initialization phase of the Simultaneous Localization and Mapping procedure, capturing the moment when the robot begins forming a partial spatial representation of its environment using early LiDAR measurements. At this stage, the mapped region is confined to one side of the environment, indicating that the exploration trajectory remains limited in spatial extent. The visible red point clusters correspond to raw range observations transformed into the global coordinate frame through incremental pose estimation derived from odometry integration. Because the robot has not yet completed significant traversal, the resulting map remains sparse and structurally incomplete, with only partial wall segments reconstructed.

The fragmented vertical boundaries illustrate the combined effects of sensor noise, discretization artifacts, and short-term pose uncertainty that commonly arise before loop closure detection and back-end optimization are activated. Small misalignments between consecutive scan segments are observable, yet the overall geometric orientation of walls remains consistent, suggesting that the front-end scan registration process is functioning correctly. The uncharted open region on the right side of the map represents unexplored territory, which is typical during frontier-based exploration in early SLAM iterations. Importantly, despite the limited spatial coverage, the reconstructed structure maintains basic geometric coherence, demonstrating effective integration between ego-motion estimation and LiDAR scan matching. These results confirm the validity of the proposed measurement model and pose propagation mechanism during the system's initialization phase, providing a stable foundation for subsequent mapping expansion and global refinement.

Fig. 11 presents the final Simultaneous Localization and Mapping output obtained after the robot completed systematic exploration of all accessible rooms within the experimental indoor environment. In contrast to the initialization stage, the reconstructed map now forms a closed and spatially coherent layout, where both external boundaries and internal partitions are distinctly represented by dense red point clusters. The upper rectangular region and the interconnected lower rooms are reconstructed with high geometric fidelity, indicating that successive LiDAR scans were accurately registered and aligned throughout the traversal. The continuity of wall structures across different sections of the environment reflects stable incremental pose estimation combined with effective global optimization. This demonstrates that accumulated odometry drift was successfully mitigated through loop closure detection and back-end refinement. Although minor variations in boundary thickness are observable, these can be attributed to measurement noise, angular resolution limits, and discretization artifacts inherent in point cloud processing. Importantly, no significant structural distortions or discontinuities are visible, confirming that the mapping framework maintained spatial consistency over extended motion sequences.

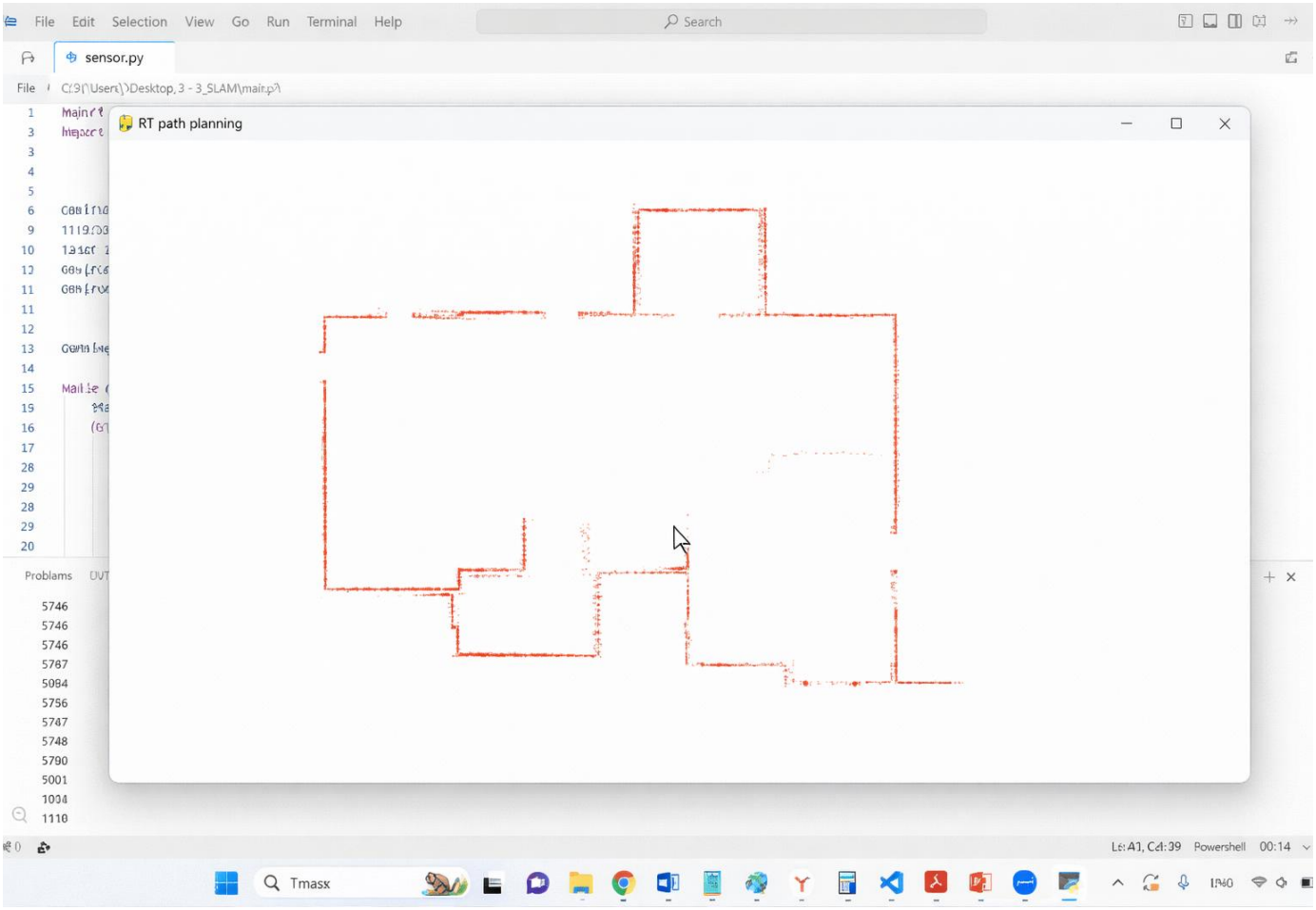

Fig. 11. Completed indoor environment reconstruction after full SLAM exploration.

Furthermore, the clear separation between adjacent rooms and the preservation of orthogonal wall geometry validate the robustness of the obstacle segmentation and occupancy updating mechanisms integrated into the mapping pipeline. Structural edges remain sharply defined even in regions with multiple scan overlaps, which suggests effective data fusion and noise filtering. The uniform distribution of mapped points across the explored area indicates sufficient environmental coverage and a balanced exploration strategy. The successful reconstruction of narrow corridors and connecting passageways further demonstrates the reliability of scan matching under constrained spatial conditions. From a navigation standpoint, the resulting map provides a dependable geometric foundation for global path planning and local obstacle avoidance. The absence of map tearing or misalignment artifacts ensures that planned trajectories will be spatially consistent with real-world geometry. Overall, the results confirm that the proposed LiDAR-based SLAM framework delivers accurate and stable large-scale indoor mapping performance, supporting reliable autonomous operation within structured environments.

Fig. 12 illustrates the experimental validation of the proposed obstacle avoidance strategy in a real indoor environment populated with multiple static obstacles. The mobile robot operates within a confined room where yellow containers are deliberately arranged to create a structured yet nontrivial navigation scenario involving narrow passages and angular turns. The spatial distribution of obstacles forces the robot to continuously perceive, localize, and re-plan its trajectory while maintaining safe clearance distances. The absence of collisions and the stable posture of the robot during maneuvering demonstrate the effectiveness of the integrated LiDAR-based perception and path planning modules. The robot successfully navigates between closely spaced obstacles, indicating accurate environmental representation and reliable obstacle boundary detection. Furthermore, the smooth trajectory adjustments observed during traversal suggest that the local planner effectively balances goal convergence and collision avoidance constraints. The experiment confirms that the proposed navigation framework maintains real-time responsiveness under indoor operational conditions. These results validate the robustness of the system in handling cluttered environments, supporting its applicability to practical deployment scenarios where dynamic decision-making and safe autonomous mobility are required.

A vertically mounted sensing mast positioned on the upper chassis carries a three-dimensional LiDAR unit that provides continuous range measurements of the surrounding environment. This sensor generates dense point cloud data for simultaneous localization, mapping, and obstacle detection. Complementing the LiDAR system, an onboard vision sensor

captures visual information to support image-based localization, object recognition, and potential semantic mapping tasks. The spatial separation of these sensors ensures a wide field of view and minimizes occlusion during forward motion. Sensor data are processed by an embedded computing module responsible for real-time sensor fusion, state estimation, and terrain evaluation.

Fig. 12. Experimental validation of real-time obstacle avoidance in a cluttered indoor environment.

The modular hardware architecture, including organized wiring and accessible mounting interfaces, indicates a design optimized for rapid prototyping and algorithm testing. The integration of both exteroceptive sensors, such as LiDAR and camera, and proprioceptive components, including joint encoders and inertial measurements, enables comprehensive perception and motion feedback. This unified platform supports simultaneous evaluation of locomotion control, real-time mapping, and collision avoidance strategies [37]. Overall, the system demonstrates a cohesive integration of mechanical design, sensing, and computational intelligence, providing a robust experimental testbed for advanced autonomous navigation research in structured and semi-structured environments.

Fig. 13 illustrates the integrated real-time SLAM and navigation visualization obtained during autonomous operation within a cluttered indoor laboratory environment. The reconstructed scene is represented as a dense three-dimensional point cloud, where structural elements such as walls, furniture, and objects are clearly distinguishable through spatial clustering and color differentiation. The blue curve indicates the estimated robot trajectory, demonstrating smooth curvature and consistent pose updates throughout the exploration cycle. The green marker represents the robot's current state estimate, while local coordinate axes provide orientation information in the global reference frame. The visualization confirms successful sensor fusion between LiDAR measurements and odometry inputs, as evidenced by the coherent alignment of environmental features without noticeable global distortion. The closed-loop trajectory suggests effective loop closure detection and back-end optimization, which reduces cumulative drift and enhances global consistency. The lower-left camera feed further validates correspondence between visual perception and spatial reconstruction, supporting multimodal situational awareness. The stability of the reconstructed geometry, even in regions containing dense objects and irregular surfaces, indicates robust scan registration and obstacle segmentation performance. Overall, the results demonstrate reliable mapping accuracy, trajectory estimation stability, and real-time computational capability suitable for autonomous navigation in complex indoor environments.

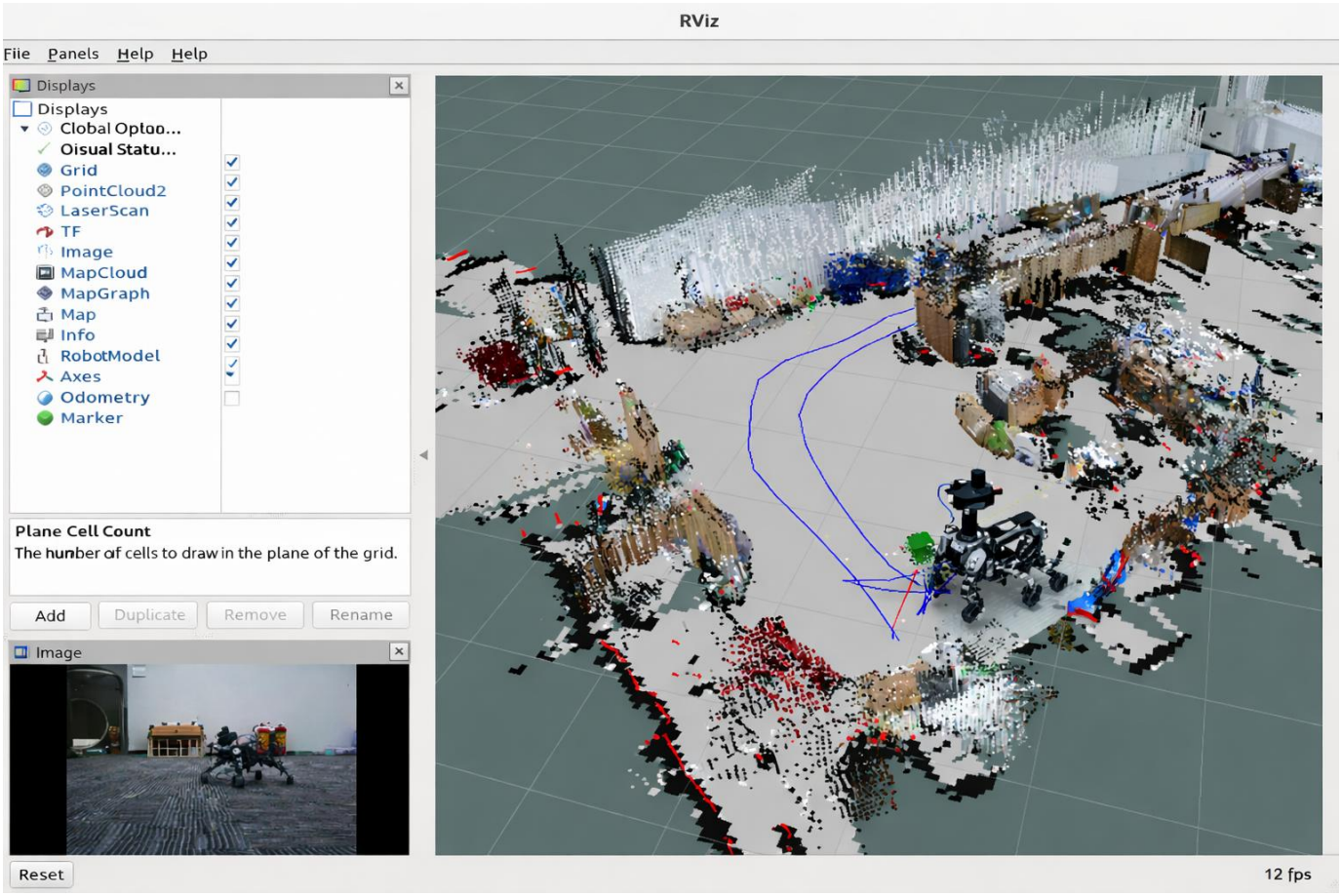

Fig. 13. Real-time 3D SLAM visualization and trajectory estimation in an indoor laboratory environment.

V. Discussion

The experimental results demonstrate that the proposed LiDAR-based SLAM and navigation framework achieves stable and geometrically consistent performance in structured indoor environments while maintaining real-time computational capability. The incremental mapping sequences confirm that the front-end scan registration and ego-motion estimation produce coherent local pose updates even during early-stage exploration [38]. Although minor discontinuities appear during initialization due to sensor noise and limited overlap between scans, the subsequent global optimization phase effectively reduces accumulated drift [39]. The full-room reconstruction results validate the robustness of the back-end optimization strategy, where loop closure detection significantly enhances global map consistency and preserves structural orthogonality of walls and partitions.

From a navigation perspective, the integration between mapping and path planning modules plays a decisive role in achieving collision-free mobility. The obstacle avoidance experiments indicate that the local planner successfully balances goal-directed motion and safety constraints in cluttered environments. The generated trajectories exhibit smooth curvature transitions, suggesting that the cost function formulation effectively penalizes abrupt steering changes while preserving feasible kinematic constraints [40]. The robot maintains stable clearance distances when navigating narrow passages, which confirms reliable obstacle boundary extraction from the LiDAR point cloud. These findings highlight the importance of accurate environmental representation for downstream motion planning performance.

The multimodal perception configuration further enhances system reliability. The combination of LiDAR sensing with odometry and optional visual input improves state estimation accuracy and environmental awareness. The 3D mapping visualization demonstrates that structural elements remain spatially aligned after loop traversal, indicating that the sensor fusion mechanism mitigates cumulative error propagation. In addition, the experimental walking robot platform validates the adaptability of the proposed framework beyond wheeled platforms [41]. The stability of locomotion combined with consistent pose estimation suggests that the algorithmic pipeline is hardware-agnostic and suitable for different robotic morphologies.

Despite the positive outcomes, several limitations deserve attention. First, the experiments were conducted in predominantly static indoor environments. Dynamic obstacle interaction was not extensively evaluated, which may affect performance under rapidly changing conditions. Second, computational scalability under large-scale outdoor scenarios requires further investigation, particularly regarding memory consumption and real-time map updates [42]. Third, although loop closure improves global consistency, false-positive

detections in visually repetitive environments could introduce pose correction artifacts. Future research should therefore focus on adaptive thresholding for loop closure verification and integration of semantic filtering to enhance robustness in complex scenes.

Overall, the discussion confirms that the proposed framework achieves a balanced trade-off between mapping accuracy, trajectory stability, and computational efficiency. The experimental validation across simulation and physical platforms demonstrates practical applicability for autonomous navigation in indoor environments. The integration of SLAM, obstacle detection, and path planning into a unified architecture provides a solid foundation for further development toward fully autonomous robotic systems capable of operating in semi-structured and unstructured environments.

VI. Conclusion

This study presented a comprehensive LiDAR-based SLAM-driven navigation framework integrating real-time mapping, obstacle avoidance, and path planning for autonomous mobile robots operating in structured indoor environments. The proposed system combines robust scan registration, pose estimation refinement, loop closure optimization, and collision-aware trajectory generation within a unified architecture. Experimental results obtained from both incremental and full-environment mapping scenarios demonstrated high geometric consistency, reduced drift accumulation, and reliable obstacle boundary extraction. The navigation experiments further validated smooth trajectory generation and stable clearance maintenance in cluttered spaces, confirming the effectiveness of the integrated planning module. The implementation on a physical robotic platform, including a walking robot equipped with LiDAR and complementary sensors, highlighted the adaptability of the framework across different hardware configurations. The system maintained real-time performance while ensuring accurate environmental reconstruction and stable localization. Although further evaluation in dynamic and large-scale outdoor environments remains necessary, the findings substantiate the robustness, scalability, and practical applicability of the proposed approach. Overall, the developed framework provides a reliable foundation for autonomous robotic navigation, supporting safe mobility and consistent environmental awareness in complex operational settings.

This research was supported by funding from the Science Committee of the Ministry of Science and Higher Education of the Republic of Kazakhstan (Project No. AP14870662)

References

[1] Nandikolla, V. K., & Ghoslin, B. (2023). Obstacle Avoidance for Omnidirectional Mobile Robot Using SLAM. Journal of Engineering and Science in Medical Diagnostics and Therapy, 6(1), 011003.

[2] Yuan, R., Ji, B., Gao, Y., & Tao, H. (2025). A review of LiDAR simultaneous localization and mapping techniques for multi-robot. Robotica, 1-41.

[3] Messbah, H., Emharraf, M., Saber, M., & Al Kaddouri, H. (2024, May). Sensor fusion using LiDAR and visual sensor for SLAM indoor navigation. In International Conference on Electronic Engineering and Renewable Energy Systems (pp. 321-331). Singapore: Springer Nature Singapore.

[4] Moshayedi, A. J., Roy, A. S., Karan, U., jun ZHANG, M., & Bassir, D. (2026). An Integrated Beetle Antennae Search–Enabled Navigation Framework for Omnidirectional AGV Mobile Robots in Unknown Environments. EAI Endorsed Transactions on AI and Robotics, 5.

[5] Chang, C. Y., Wu, C. L., Cheng, J. M., & Jian, S. J. (2023). Autonomous mobile robots for recycling metal shaving at CNC factories. The International Journal of Advanced Manufacturing Technology, 126(5), 2205-2218.

[6] Omarov, B., Batyrbekov, A., Dalbekova, K., Abdulkarimova, G., Berkimbaeva, S., Kenzhegulova, S., ... & Omarov, B. (2020, December). Electronic stethoscope for heartbeat abnormality detection. In International Conference on Smart Computing and Communication (pp. 248-258). Cham: Springer International Publishing.

[7] Zulkifli, A. T., Tomari, M. R. M., & Zakaria, W. N. W. (2023). Lidar based autonomous navigation for usv pipeline inspection. Evolution in Electrical and Electronic Engineering, 4(1), 337-346.

[8] Tsanko, A., Kansizoglou, I., Bampis, L., & Gasteratos, A. (2025, October). Simulation-Driven Development of a Custom Mobile Manipulator for RoboCup@ Work. In 2025 IEEE International Conference on Imaging Systems and Techniques (IST) (pp. 1-6). IEEE.

[9] Gan, V. J. (2025). Robot-Assisted 3D Scene Reconstruction Using Fixed FOV LiDAR-Based Depth Camera. In ISARC. Proceedings of the International Symposium on Automation and Robotics in Construction (Vol. 42, pp. 288-295). IAARC Publications.

[10] Jian, Z., Lu, Z., Zhou, X., Lan, B., Xiao, A., Wang, X., & Liang, B. (2022, October). Putn: A plane-fitting based uneven terrain navigation framework. In 2022 IEEE/RSJ International Conference on Intelligent Robots and Systems (IROS) (pp. 7160-7166). IEEE.

[11] Čičiurėnas, D., Zulkifal, M., & Bučinskas, V. (2024). Conception of the Channel Robot Navigation. Automation 2024: Advances in Automation, Robotics and Measurement Techniques, 192.

[12] M. Tehrani, B., BuHamdan, S., & Alwisy, A. (2023). Robotics in assembly-based industrialized construction: A narrative review and a look forward. International Journal of Intelligent Robotics and Applications, 7(3), 556-574.

[13] Omarov, B., Omarov, B., Rakhymzhanov, A., Niyazov, A., Sultan, D., & Baikuvekov, M. (2024). Development of an artificial intelligence-enabled non-invasive digital stethoscope for monitoring the heart condition of athletes in real-time. Retos, 60, 1169-1180.

[14] Jardali, H., Ali, M., & Liu, L. (2024, May). Autonomous mapless navigation on uneven terrains. In 2024 IEEE International Conference on Robotics and Automation (ICRA) (pp. 13227-13233). IEEE.

[15] Müller, J., Trattnig, S., Heuss, L., Geng, P., Tanz, L., & Daub, R. (2025, August). Automated Workspace Scanning with Local Areas of Interest in the Context of Industrial Robots as a Service (IRaaS). In 2025 IEEE 21st International Conference on Automation Science and Engineering (CASE) (pp. 1219-1224). IEEE.

[16] Ildirimzade, M. A. (2025). Advancement in Autonomous Navigation in Space through Artificial Intelligence: A Systematic Review. London Journal of Research In Computer Science and Technology, 25(1), 21-33.

[17] Ejidokun, T. O., Omitola, O. O., Fiyinfoluwa, A., Onodjohwo, S., Odoguwu, C., & Odoguwu, C. (2022). A Conceptual Design of a Vision-Based Fire Fighting Robot for Smart City Application. Journal Européen des Systèmes Automatisés, 55(3), 299-305.

[18] Chen, T., Shorinwa, O., Bruno, J., Swann, A., Yu, J., Zeng, W., ... & Schwager, M. (2025). Splat-nav: Safe real-time robot navigation in gaussian splatting maps. IEEE Transactions on Robotics.

[19] Chen, J., Gugssa, M., Yee, J., Wang, J., Goodin, C., & Das, A. R. (2023, June). Framework for digital twin creation in off-road environments from LiDAR scans. In Synthetic Data for Artificial Intelligence and Machine Learning: Tools, Techniques, and Applications (Vol. 12529, pp. 117-128). SPIE.

[20] Yue, H., Sun, Y., Zeng, N., Chen, S., Tan, Y., & Wang, Q. (2025). Legged robots for construction management: Applications and challenges. Journal of Construction Engineering and Management, 151(8), 03125006.

[21] Jing, Y., Haowei, M., Ansari, A. S., Sucharitha, G., Omarov, B., Kumar, S., ... & Alyamani, K. A. (2023). Soft computing techniques for detecting cyberbullying in social multimedia data. ACM Journal of Data and Information Quality, 15(3), 1-14.

[22] Sifat, A. H., Bharmal, B., Zeng, H., Huang, J. B., Jung, C., & Williams, R. K. (2023). Towards computational awareness in autonomous robots: an empirical study of computational kernels. Complex & Intelligent Systems, 9(6), 6269-6295.

[23] Wei, G., Liu, J., Zeng, Y., Li, S., Teng, W., Li, R., ... & Ma, X. (2025). Robotic Floor Nailing of a Modular Container Building Structural Assembly Based on Multilevel Localization and Active Planning. Journal of Computing in Civil Engineering, 39(6), 04025101.

[24] Gopee, M. A., Prieto, S. A., & García de Soto, B. (2023). Improving autonomous robotic navigation using IFC files. Construction Robotics, 7(3), 235-251.

[25] Liu, J., Wei, G., Cheng, G. Z., Zeng, Y., Li, S., Li, R., ... & Teng, W. Robotic Floor Nailing of Modular Container Building Decoration Based on Two-Stage Location and Active Planning. Available at SSRN 4654625.

[26] Wei, W., Ghafarian, M., Shirinzadeh, B., Al-Jodah, A., & Nowell, R. (2022). Posture and map restoration in slam using trajectory information. Processes, 10(8), 1433.

[27] Kim, Y., Chen, Y., Gombolay, M., & Cho, Y. K. (2025). Understanding the effects of humanlike robot motions on unfocused human–robot interaction. Advanced Engineering Informatics, 68, 103751.

[28] Chen, K., Xiao, J., Liu, J., Tong, Q., Zhang, H., Liu, R., ... & Chen, S. (2025). Semantic visual simultaneous localization and mapping: A survey. IEEE Transactions on Intelligent Transportation Systems.

[29] Naskar, A., Pothapragada, P., & Vivekananda Shanmuganathan, P. (2023, December). Digital Twin-Based Path Planning and Obstacle Avoidance for a Quadruped Robot. In International and National Conference on Machines and Mechanism (pp. 673-684). Singapore: Springer Nature Singapore.

[30] Abdelsalam, A., Happonen, A., Kärhä, K., Kapitonov, A., & Porras, J. (2022). Toward autonomous vehicles and machinery in mill yards of the forest industry: Technologies and proposals for autonomous vehicle operations. IEEE Access, 10, 88234-88250.

[31] Liu, Y., Min, Y., Xu, W., Du, J., & Wei, Z. (2023, February). Integrated Sensing and Communication in Obstacle Avoidance System for Autonomous Vehicles. In 2023 International Conference on Intelligent Computing and Control (IC&C) (pp. 90-97). IEEE.

[32] Liang, H., Yeoh, J. K., & Chua, D. K. (2024). Premapping of dynamic indoor construction sites using prior construction progress video to enhance UGV path planning. Journal of Computing in Civil Engineering, 38(5), 04024025.

[33] Gao, W., & Li, G. (2024). Typical engineering applications of 3d point clouds. In Deep Learning for 3D Point Clouds (pp. 273-299). Singapore: Springer Nature Singapore.

[34] Wu, H., Liu, Y., Chang, R., & Wu, L. (2024). Research status quo and trends of construction robotics: A bibliometric analysis. Journal of Computing in Civil Engineering, 38(1), 03123001.

[35] Mabkhot, M. M., Flanagan, M., Bahraini, M. S., Yu, Y., Sun, C., Coombes, M., ... & Lohse, N. (2024). Technical and system requirements for industrial robot-as-a-service (IRaaS). Procedia CIRP, 130, 816-823.

[36] Avutu, S. R., Paul, S., & Reddy, B. V. (2023). A review on wheelchair and add-in devices design for the disabled. International Journal of Biomedical Engineering and Technology, 41(1), 35-59.

[37] Cabrera, J. J., Cebollada, S., Flores, M., Reinoso, Ó., & Payá, L. (2022). Training, optimization and validation of a CNN for room retrieval and description of omnidirectional images. SN Computer Science, 3(4), 271.

[38] Yao, Q., Mao, C., Wang, T., Zhang, B., Yan, R., & Sun, B. (2025). Evaluating framework for the capability of construction robots. Engineering, Construction and Architectural Management.

[39] Zhang, Y., Wang, Z., Wang, X., Gao, P., & Li, M. (2024). A 3D pickup estimation method for industrial parallel robots based on point cloud simplification and registration. The International Journal of Advanced Manufacturing Technology, 133(11), 5175-5195.

[40] Al Noman, M. A., Zhai, L., Almukhtar, F. H., Rahaman, M. F., ... & Wang, C. (2023). A computer vision-based lane detection technique using gradient threshold and hue-lightness-saturation value for an autonomous vehicle. International Journal of Electrical and Computer Engineering, 13(1), 347.

[41] Wang, K., Antwi-Afari, M. F., Ossei-Gudom, B. M., Yi, W., Li, J., & Banihashemi, S. (2025). Recent advances in virtual reality applications for construction safety management. Construction Innovation.

[42] Wang, M., Cai, J., Hu, D., Hu, Y., Han, Z., & Li, S. (2025). AI-based robots in industrialized building manufacturing. Frontiers of Engineering Management, 12(1), 59-85.